61-3; $LMn^{III}Cl$, 137203-62-4; $LMn^{III}NCS$, 137203-63-5; $LMn^{III}N_3$, 137203-64-6; $[(LH)_2Zn_2(\mu\text{-}OH)](ClO_4)$, 137203-60-2; $[(LH)_2Zn_2(\mu\text{-}OH)](PF_6)\cdot 0.5CH_3OH$, 137331-20-5; $[LZn(H_2O)ZnCl_2]\cdot 0.5CH_3CN$, 137203-66-8; 1-oxa-4,7-diazacyclononane, 80289-59-4; 2-(bromomethyl)phenyl acetate, 704-65-4; 4,7-bis(2-(acetyloxy)benzyl)-1-oxa-4,7-diazacyclononane, 137203-55-5.

Supplementary Material Available: Listings of crystallographic data, calculated positions and thermal parameters of hydrogen atoms, bond lengths and bond angles, and anisotropic thermal parameters for $[(LH)_2Zn_2(\mu\text{-}OH)](PF_6)\cdot 0.5CH_3OH$ (6 pages); a table of structure factors (18 pages). Ordering information is given on any current masthead page.

Contribution from the Department of Chemistry, Waseda University, Tokyo 169, Japan, Department of Chemistry, Toho University, Funabashi, Chiba 274, Japan, and Instrumental Analysis Center of Chemistry, Faculty of Science, Tohoku University, Aramaki Aoba, Aoba-ku, Sendai 980, Japan

Syntheses, Structures, and Reactivities of the Sulfur-Bridged Trinuclear Complexes $[(L)Ru(CO)(PPh_3)]_2(\mu\text{-}MS_4)$ (L = PhNCHS, $CH_2CH_2(C_5H_4N)$, $CH_2CH_2C(O)OMe$; M = Mo, W). Photochemical and Chemical Reactions and Isolation of a Trinuclear Complex Having a Coordinatively Unsaturated Ruthenium Atom

Masao Kato,[1a] Masaki Kawano,[1a] Hirokazu Taniguchi,[1a] Mikimasa Funaki,[1a] Hiroshi Moriyama,[1b] Toshio Sato,[1c] and Kazuko Matsumoto*,[1a]

Received January 3, 1991

Syntheses, structures, and reactivities of the title compounds are reported. $[(PhNCHS)Ru(CO)(PPh_3)]_2(\mu\text{-}MS_4)\cdot 2(CH_3)_2CO$ (M = Mo (**1**) and M = W (**3**)) undergoes photochemical reaction in the presence of pyridine (py) to afford $[(PhNCHS)Ru(py)_2]_2(\mu\text{-}MS_4)$ and $[(PhNCHS)Ru(py)_2](\mu\text{-}MS_4)[(PPh_3)(CO)Ru(PhNCHS)]$. In the reaction with Me_3NO, **1** and **3** give $[(PhNCHS)Ru(PPh_3)](\mu\text{-}MS_4)[(PPh_3)(CO)Ru(PhNCHS)]$, which has a novel five-coordinated Ru atom. This reaction product further undergoes chemical reaction in the presence of py to give $[(PhNCHS)Ru(py)_2]_2(\mu\text{-}MS_4)$. Compound **1** crystallizes in the orthorhombic space group *Pbcn* with a = 30.692 (4) Å, b = 8.735 (2) Å, c = 22.302 (4) Å, V = 5980 (2) Å^3, and Z = 4. Anisotropic refinement of all non-hydrogen atoms converged to the residuals R = 0.065 and R_w = 0.072 ($w = 1/\sigma^2(F)$). Compound **3** crystallizes in the same space group as **1** with a = 30.826 (7) Å, b = 8.735 (3) Å, c = 22.306 (4) Å, V = 6000 (3) Å^3, and Z = 4. The final R values were R = 0.080 and R_w = 0.090 ($w = 1/\sigma^2(F)$).

Introduction

We have attempted to synthesize sulfur-bridged cluster complexes that are robust against ligand substitution, leading to the reactions of coordinated small ligand molecules like nitrogen-fixing enzymes.[2-6] The scope of our research is not limited to the metals relevant to the enzymes but is expanded generally to other metals for constructing cluster frameworks that can endure a wide variety of substitution and redox reactions. In this respect, ruthenium seems advantageous because of its strong π-back-donating ability. In the present study two ruthenium atoms are bridged by MS_4^{2-} (M = Mo, W) to form trinuclear cluster complexes. Although MS_4^{2-} compounds have widely been studied as ligands for many transition metals in possible relevance to the biological molecules and a number of binuclear or trinuclear complexes of the type $L_2M'(MS_4)$,[7] $M'(MS_4)_2$,[8-10] and $(M'L_n)_2(\mu\text{-}MS_4)$[11,12] (M' is the transition element) have been reported, research has still been limited for the employment of MS_4^{2-} as ligands to simple coordination compounds and only a few compounds are reported where MS_4^{2-} is coordinated to organometallic groups. We have been interested in the reactivities of organoruthenium cluster complexes involving MS_4^{2-} and report here the first realization of photochemical or chemical dissociation of a coordinated carbonyl group to produce a five-coordinated ruthenium atom. MS_4^{2-}-bridged trimetallic complexes with a $Ru(\mu\text{-}MS_4)Ru$ framework and basic ligand substitution reactions have already been reported for other $Ru(\mu\text{-}MS_4)Ru$ compounds.[13-15] However, the present report is the first example of photochemical substitution in Ru and any other $(M'L_n)_2(\mu\text{-}MS_4)$ complexes.

Experimental Section

Preparation of the Complexes. All compounds described herein are air-stable, except those containing a five-coordinated Ru atom. The latter

(1) (a) Waseda University. (b) Toho University. (c) Tohoku University.
(2) Holm, R. H. *Chem. Soc. Rev.* **1981**, *10*, 455.
(3) Coucouvanis, D. *Acc. Chem. Res.* **1981**, *14*, 201.
(4) Zumft, W. G. *Eur. J. Biochem.* **1978**, *91*, 345.
(5) Palermo, R. E.; Singh, R.; Bashkin, J. K.; Holm, R. H. *J. Am. Chem. Soc.* **1984**, *106*, 2600.
(6) Holm, R. H.; Simhon, E. D. In *Molybdenum Enzymes*: Spiro, T. G., Ed.; Wiley Interscience: New York, 1985; Chapter 1.
(7) Siedel, A. R.; Hubbard, C. R.; Mighell, A. D.; Doherty, R. M.; Stewart, J. M. *Inorg. Chim. Acta* **1980**, *38*, 197.
(8) Bowmarker, G. A.; Boyd, P. D. W.; Sorrenson, R. J.; Reed, C. A.; McDonald, J. W. *Inorg. Chem.* **1985**, *24*, 3.
(9) (a) $M'(MS_4)_2^{2-}$ (M' = Ni, Pd, Pt): Callahan, K. P.; Piliero, P. A. *Inorg. Chem.* **1980**, *19*, 2619. (b) $Fe(WS_4)_2^{2-}$: Stremple, P.; Baenziger, N. C.; Coucouvanis, D. *J. Am. Chem. Soc.* **1981**, *103*, 4601. (c) $Co(WS_4)_2^{2-/3-}$: Muller, A.; Hellmann, W.; Schimanski, U.; Jostes, R.; Newton, W. E. *Z. Naturforsch., B: Anorg. Chem., Org. Chem.* **1983**, *38*, 528. Muller, A.; Jostes, R.; Flemming, V.; Potthast, R. *Inorg. Chim. Acta* **1980**, *44*, L33.
(10) (a) $Mo_2S_6^{2-}$, $Mo_2S_7^{2-}$, and $Mo_2S_9^{2-}$: Coucouvanis, D.; Hadjikyriacou, A. *Inorg. Chem.* **1987**, *26*, 1. (b) $W_4S_{12}^{2-}$: Secheresse, F.; LeFebvre, J.; Daran, J. C.; Jeannin, Y. *Inorg. Chem.* **1982**, *21*, 1311. (c) $W_3S_9^{2-}$: Cohen, S. A.; Stiefel, E. I. *Inorg. Chem.* **1985**, *24*, 4657. (d) $W_3S_8^{2-}$: Bhaduri, S.; Ibers, J. A. *Inorg. Chem.* **1986**, *25*, 3.
(11) Do, Y.; Simhon, E. D.; Holm, R. H. *Inorg. Chem.* **1985**, *24*, 4635.
(12) (a) $(FeCl_2)_2WS_4^{2-}$: Coucouvanis, D.; Simhon, E. D.; Stremple, P.; Ryan, M.; Swenson, D.; Baenziger, N. C.; Simopoulos, A.; Papaefthymiou, V.; Kostikas, A.; Petrouleas, V. *Inorg. Chem.* **1984**, *23*, 741. (b) $Au_2(PPh_3)_nMoS_4$ (n = 2, 3): Charnock, J. M.; Bristow, S.; Nicholson, J. R.; Garner, C. D.; Clegg, W. *J. Chem. Soc., Dalton Trans.* **1987**, *303*. (c) $Au_2(PEt_3)_2MoS_4$: Kinsch, E. M.; Stephan, D. W. *Inorg. Chim. Acta* **1985**, *96*, L87. (d) Manoli, J. M.; Potvin, C.; Secheresse, F.; Marzak, S. *J. Chem. Soc., Chem. Commun.* **1986**, 1557.
(13) Howard, K. E.; Rauchfuss, T. B.; Wilson, S. R. *Inorg. Chem.* **1988**, *27*, 1710.
(14) Greaney, M. A.; Coyle, C. L.; Harmer, M. A.; Jordan, A.; Stiefel, E. I. *Inorg. Chem.* **1989**, *28*, 912.
(15) Tanaka, K.; Morimoto, M.; Tanaka, T. *Inorg. Chim. Acta* **1981**, L61.

0020-1669/92/1331-0026$03.00/0

complexes are unstable at room temperature and the powder sample should be stored in an inert atmosphere in a refrigerator. The solution is much more unstable, and the compound gradually decomposes even in a refrigerator. All reactions were carried out in air unless otherwise stated. All solvents were reagent grade and were used without further purification. $(PPh_4)_2MS_4$ (M = Mo, W),[16] the Ru–*N*-phenylthioformamide complex RuCl(PhNCHS)(CO)$(PPh_3)_2$,[17] the Ru–vinylpyridine complex RuCl{$CH_2CH_2(C_5H_4N)$}(CO)$(PPh_3)_2$,[18] and the Ru–methylacrylate complex RuCl{$CH_2CH_2C(O)OMe$}(CO)$(PPh_3)_2$[18] were prepared by literature methods.

[(PhNCHS)Ru(CO)(PPh_3)]$_2(\mu$-$MoS_4)$ (1). A suspension of 0.5 g (0.6 mmol) of RuCl(PhNCHS)(CO)$(PPh_3)_2$ and 0.27 g (0.3 mmol) of $(PPh_4)_2MoS_4$ in 30 mL of *n*-$CH_3(CH_2)_2CN$ were refluxed for 30 min under N_2. The suspension gradually turned from orange yellow to a clear red solution during the refluxing, which was filtered and was concentrated to ca. 10 mL under reduced pressure. To the solution was added 50 mL of 2-propanol/*n*-hexane (1:1 v/v) to precipitate a red powdery material. The precipitate was recrystallized from $CH_2Cl_2/(CH_3)_2CO$ (1:1 v/v) (yield 75%). Anal. Calcd for $C_{52}H_{42}N_2O_2P_2S_6MoRu_2$: C, 48.82; H, 3.31; N, 2.19; S, 15.04. Found: C, 48.63; H, 3.45; N, 2.08; S, 14.56. IR (KBr pellet): 462 (s), 424 (w), 1973 (s), 692 (s), 744 (m), 880 (w), 914 (w), 1092 (m) cm^{-1}. FABMS: *m/e* 1280 (M + H^+), 1252 (M^+ – CO), 1145 (M^+ – PhNCHS), 1116 (M^+ – CO – PhNCHS), 1087 (M^+ – 2CO – PhNCHS), 983 (M^+ – CO – 2PhNCHS), 964 (M^+ – 2CO – 2PhNCHS), 825 (M^+ – 2CO – PhNCHS – PPh_3), 720 (M^+ – CO – 2PhNCHS – PPh_3). ^1H NMR: S–CH–N, δ 8.45 (d), $^4J_{P-H}$ = 2.93 Hz; δ 5.93–7.63 (m). The crystal used for the X-ray diffraction study was obtained as the solvated compound [(PhNCHS)Ru(CO)(PPh_3)]$_2$-(MoS_4)·2$(CH_3)_2CO$ by the recrystallization of **1** from acetone.

[(PhNCHS)Ru(CO)(PPh_3)]$_2(\mu$-$WS_4)$ (2). The compound was prepared in exactly the same way as for **1**. An orange powder was obtained. Anal. Calcd for $C_{52}H_{42}N_2O_2P_2S_6WRu_2$: C, 45.68; H, 3.10; N, 2.05. Found: C, 46.04; H, 3.57; N, 2.05. The yield was 67%. IR (KBr pellet): 447 (s), 424 (sh), 1977 (s), 689 (s), 745 (m), 879 (w), 915 (w), 1093 (m) cm^{-1}. FABMS: *m/e* 1368 (M + H^+), 1340 (M^+ – CO), 1204 (M^+ – PhNCHS), 1175 (M^+ – CO – PhNCHS), 1070 (M^+ – CO – 2PhNCHS), 912 (M^+ – CO – PhNCHS – PPh_3), 809 (M^+ – CO – 2PhNCHS – PPh_3). ^1H NMR: S–CH–N, δ 8.50 (d), $^4J_{P-H}$ = 2.44 Hz; δ 5.95–7.62 (m).

[(PhNCHS)Ru(CO)(PPh_3)]$_2(\mu$-$WS_4)$·2$(CH_3)_2CO$ (3). The compound was obtained as orange parallelepiped crystals on recrystallization of **2** from acetone. The existence of the acetone molecules was confirmed by ^1H NMR spectroscopy of a $CDCl_3$ solution of **3**. Anal. Calcd for $C_{58}H_{54}N_2O_4P_2S_6WRu_2$: C, 46.96; H, 3.67; N, 1.89. Found: C, 46.45; H, 3.48; N, 1.91.

[{$CH_2CH_2(C_5H_4N)$}Ru(CO)(PPh_3)]$_2(\mu$-$MoS_4)$ (4). A suspension of 0.48 g (0.6 mmol) of RuCl{$CH_2CH_2(C_5H_4N)$}(CO)$(PPh_3)_2$ and 0.27 g (0.3 mmol) of $(PPh_4)_2MoS_4$ in 30 mL of *n*-$CH_3(CH_2)_2CN$ were heated at 90 °C under N_2 for 2 h. The suspension gradually turned from greenish yellow to a clear red solution, which was filtered and was concentrated to ca. 10 mL under reduced pressure. Fifty milliliters of 2-propanol/*n*-hexane (1:1 v/v) was added to the solution to precipitate a red powder. The precipitate was purified by column chromatography on neutral Al_2O_3 by using benzene and ethylacetate (9:1 v/v) as eluent. Concentration of the eluate afforded the red powder of **4**. Anal. Calcd for $C_{52}H_{46}N_2O_2P_2S_4MoRu_2$: C, 51.23; H, 3.80; N, 2.30. Found: C, 51.16; H, 3.87; N, 2.24. The yield was 81%. IR (KBr pellet): 459 (s), 436 (w), 1940 (s), 593 (m), 695 (s), 742 (m), 1027 (m) cm^{-1}. FABMS: *m/e* 1218 (M^+ – H), 1187 (M^+ – CO), 1115 (M^+ – CO – C_7H_6N).

[{$CH_2CH_2(C_5H_4N)$}Ru(CO)(PPh_3)]$_2(\mu$-$WS_4)$ (5). The compound was prepared in exactly the same way as for **4**. A yellow powder was obtained with a yield of 65%. Anal. Calcd for $C_{52}H_{46}N_2O_2P_2S_4WRu_2$: C, 47.78; H, 3.55; N, 2.14. Found: C, 47.93; H, 3.75; N, 2.07. IR (KBr pellet): 448 (s), 1936 (s), 596 (m), 695 (s), 743 (m), 1027 (m) cm^{-1}. FABMS: *m/e* 1308 (M + H^+), 1280 (M^+ – CO), 1202 (M^+ – C_7H_6N), 1173 (M^+ – CO – C_7H_6N), 1044 (M^+ – PPh_3), 1015 (M^+ – CO – PPh_3), 987 (M^+ – 2CO – PPh_3), 880 (M^+ – 2CO – C_7H_6N – PPh_3).

[{$CH_2CH_2C(O)OMe$}Ru(CO)(PPh_3)]$_2(\mu$-$MoS_4)$ (6). A suspension of 0.47 g (0.6 mmol) of RuCl{$CH_2CH_2C(O)OMe$}(CO)$(PPh_3)_2$ and 0.27 g (0.3 mmol) of $(PPh_4)_2MoS_4$ in 30 mL of *n*-$CH_3(CH_2)_2CN$ were stirred at 50 °C under N_2 for 5 h. The suspension gradually turned from greenish yellow to a clear red solution, which was filtered and concentrated to ca. 10 mL under reduced pressure. The reaction must be carried out at 50 °C, since the ruthenium starting material decomposes above 50 °C. To the concentrated solution was added 50 mL of 2-propanol/*n*-hexane (1:1 v/v), and a red precipitate was obtained. The precipitate was purified by column chromatography on neutral Al_2O_3 by using benzene and ethyl acetate (9:1 v/v) as eluent. The red powder of **6** was obtained by concentrating the eluate. The yield was 85%. Anal. Calcd for $C_{46}H_{44}O_6P_2S_4MoRu_2$: C, 46.78; H, 3.76. Found: C, 47.55; H, 3.86. IR (KBr pellet): 459 (s), 430 (w), 1945 (s), 1645 (s), 695 (s), 745 (m), 1092 (s), 1186 (m), 1223 (s), 1357 (s), 1435 (s) cm^{-1}. FABMS: *m/e* 1187 (M^+ + H), 1152 (M^+ – CO), 1094 (M^+ – $C_4H_7O_2$), 1067 (M^+ – CO – $C_4H_7O_2$), 1008 (M^+ – $2C_4H_7O_2$), 980 (M^+ – CO – $2C_4H_7O_2$), 951 (M^+ – 2CO – $2C_4H_7O_2$).

[{$CH_2CH_2C(O)OMe$}Ru(CO)(PPh_3)]$_2(\mu$-$WS_4)$ (7). The compound was prepared in the same way as for **6**. A yellow powder was obtained with a yield of 72%. Anal. Calcd for $C_{46}H_{44}O_6P_2S_4WRu_2$: C, 43.54; H, 3.50. Found: C, 44.39; H, 3.85. IR (KBr pellet): 448 (s), 1944 (s), 1647 (s), 696 (s), 745 (m), 1092 (s), 1187 (m), 1224 (m), 1357 (s), 1435 (s) cm^{-1}. FABMS: *m/e* 1270 (M^+ + H), 1242 (M^+ – CO), 1183 (M^+ – $C_4H_7O_2$), 1097 (M^+ – $2C_4H_7O_2$), 1068 (M^+ – CO – $2C_4H_7O_2$), 1039 (M^+ – 2CO – $2C_4H_7O_2$), 833 (M^+ – $2C_4H_7O_2$ – PPh_3), 805 (M^+ – CO – $2C_4H_7O_2$ – PPh_3), 777 (M^+ – 2CO – $2C_4H_7O_2$ – PPh_3).

Photochemical Synthesis of [(PhNCHS)Ru(py)$_2$]$_2(\mu$-$MS_4)$ (M = Mo (8), M = W (9)). The two compounds were prepared by the same method starting from the corresponding [(PhNCHS)Ru(CO)-(PPh_3)]$_2MS_4$, therefore the procedure for M = Mo is described here. A solution of 0.13 g (1×10^{-4} mol) of **1** in 200 mL of pyridine (py) was irradiated with a 400-W high-pressure Hg lamp for 30 min. The solution turned from red to green and finally to brown during the irradiation. After irradiation, the solution was filtered and concentrated to ca. 10 mL under reduced pressure. Fifth milliliters of diethyl ether was added to the solution, and a brown precipitate was obtained. The precipitate was purified by column chromatography on neutral Al_2O_3 by using benzene as eluent. The eluate was concentrated to ca. 10 mL under reduced pressure, and 50 mL of diethyl ether was added to precipitate the brown powder of **8**. The yield was 38%. The photochemical reaction did not proceed in pure benzene, but took place when pyridine was added. Anal. Calcd for $C_{34}H_{32}N_6S_6MoRu_2$: C, 40.23; H, 3.18; N, 8.28. Found: C, 40.87; H, 3.25; N, 8.02. ^1H NMR: S–CH–N, δ 9.94 (s); py H α, δ 8.39 (d), $^3J_{H-H}$ = 5.37 Hz, δ 8.35 (d), $^3J_{H-H}$ = 5.37 Hz; δ 6.83–7.75 (m). The green tungsten analogue **9** was obtained in a similar way. Anal. Calcd for $C_{34}H_{32}N_6S_6WRu_2$: C, 37.02; H, 2.92; N, 7.62. Found: C, 37.27; H, 2.97; N, 7.57. IR (KBr pellet): 456 (s), 692 (s), 760 (s), 916 (w), 1212 (w) cm^{-1}. FABMS: *m/e* 1016 (M^+), 935 (M^+ – C_5H_5N), 856 (M^+ – $2C_5H_5N$). ^1H NMR: S–CH–N, δ 9.95 (s); py H α, δ 8.39 (d), $^3J_{H-H}$ = 5.37 Hz, δ 8.36 (d), $^3J_{H-H}$ = 5.37 Hz; δ 6.83–7.76 (m).

Compound **8** can also be prepared by irradiating a solution of [(PhNCHS)Ru(PPh_3)]$(\mu$-$MoS_4)$[(PPh_3)(CO)Ru(PhNCHS)] (**10**) (0.13 g, 1×10^{-4} mol) in 200 mL of py for 30 min. The resulting brown solution was filtered and concentrated to ca. 10 mL under reduced pressure. Fifty milliliters of diethyl ether was added to the solution, and a brown precipitate was obtained. The precipitate was purified by column chromatography on neutral Al_2O_3 by using benzene as eluent. The eluate was concentrated to ca. 10 mL under reduced pressure, and 50 mL of diethyl ether was added to precipitate the brown powder of **8**. The yield was 29%.

Compound **8** was also prepared by irradiating a solution of [(PhNCHS)Ru$(py)_2$]$(\mu$-$MoS_4)$[(PPh_3)(CO)Ru(PhNCHS)] (**11**) (0.12 g, 1×10^{-4} mol) in 200 mL of py for 30 min. The resulting brown solution was treated in the same way as in the previous two methods, and the brown powder of **8** was obtained with a yield of 32%.

[(PhNCHS)Ru(PPh_3)]$(\mu$-$MoS_4)$[(PPh_3)(CO)Ru(PhNCHS)] (10). To a solution of 0.25 g (2×10^{-4} mol) of **1** in 50 mL of pyridine was added 0.15 g (2×10^{-3} mol) of $Me_3NO·2H_2O$. The solution was stirred at 50 °C for 4 h, during which period the solution turned from red to green, and it was concentrated to 10 mL under reduced pressure at room temperature. To the solution was added excess 2-propanol and *n*-hexane to obtain the green powder of **10**. Anal. Calcd for $C_{51}H_{42}N_2OP_2MoRu_2$: C, 48.95; H, 3.38; N, 2.24. Found: C, 49.38; H, 3.72; N, 2.44. The yield was 97%. IR (KBr pellet): 460 (s), 436 (w), 1956 (s), 694 (s), 756 (m), 886 (w), 916 (w), 1090 (m) cm^{-1}. FABMS: *m/e* 1251 (M^+), 1221 (M^+ – CO), 1115 (M^+ – PhNCHS), 1087 (M^+ – CO – PhNCHS), 983 (M^+ – 2PhNCHS), 962 (M^+ – CO – PPh_3), 853 (M^+ – PhNCHS – PPh_3), 823 (M^+ – CO – PhNCHS – PPh_3). ^1H NMR: S–CH–N δ 9.22 (s), 9.13 (s), 8.41 (t), $^4J_{P-H}$ = 2.44 Hz; δ 5.90–7.61 (m).

[(PhNCHS)Ru$(py)_2$]$(\mu$-$MoS_4)$[(PPh_3)(CO)Ru(PhNCHS)] (11). A solution containing 0.25 g (2×10^{-4} mol) of 10 in 20 mL of pyridine was refluxed for 1 h and then concentrated to 5 mL under reduced pressure. Excess of 2-propanol and *n*-hexane was added to the solution to precipitate green powder. The precipitate was purified on a neutral Al_2O_3 column with benzene as eluent. The yield was 52%. Anal. Calcd for $C_{43}H_{37}N_4OPMoRu_2$: C, 45.02; H, 3.25; N, 4.88. Found: C, 45.48; H, 3.35; N, 4.52. IR (KBr pellet): 460 (s), 430 (w), 1956 (s), 640 (s), 694

(16) Corleis, E. *Justus Liebigs Ann. Chem.* **1886**, 244.
(17) Robinso, S. D.; Sahajpal, A. *Inorg. Chem.* **1977**, *16*, 2722.
(18) Hiraki, K.; Ochi, N.; Sasada, Y.; Hayashida, H.; Fuchita, Y.; Yamanaka, S. *J. Chem. Soc., Dalton Trans.* **1985**, 873.

Table I. Summary of Crystal Data for $[(PhNCHS)Ru(CO)(PPh_3)]_2(MoS_4)\cdot 2C_3H_6O$

formula	$C_{58}H_{54}N_2O_4P_2S_6MoRu_2$	Z	4
		d_{calcd}, g cm^{-3}	1.42
fw	1395.5	d_{obsd}, g cm^{-3}	1.43
cryst syst	orthorhombic	abs coeff (μ), cm^{-1}	9.81
space group	*Pbcn* (No. 60)	radiation (λ, Å)	Mo Kα (0.71068)
a, Å	30.692 (4)	R	0.065
b, Å	8.735 (2)	R_w	0.072
c, Å	22.302 (4)	GOF	1.58
V, Å^3	5980 (2)		

Table II. Summary of Crystal Data for $[(PhNCHS)Ru(CO)(PPh_3)]_2(WS_4)\cdot 2C_3H_6O$

formula	$C_{58}H_{54}N_2O_4P_2S_6Ru_2W$	Z	4
		transm factors	1.00–0.86
fw	1483.4	d_{calcd}, g cm^{-3}	1.52
cryst syst	orthorhombic	d_{obsd}, g cm^{-3}	1.52
space group	*Pbcn* (No. 60)	abs coeff (μ), cm^{-1}	28.11
a, Å	30.826 (7)	radiation (λ, Å)	Mo Kα (0.71068)
b, Å	8.735 (3)	R	0.080
c, Å	22.306 (4)	R_w	0.090
V, Å^3	6000 (3)	GOF	1.36

Table III. Positional and Thermal Parameters for $[(PhNCHS)Ru(CO)(PPh_3)]_2(MoS_4)\cdot 2C_3H_6O$

atom	x/a	y/b	z/c	B, Å^2
Mo	0.0	−0.1101 (2)	0.25	3.06 (3)
Ru	−0.08485 (3)	−0.1025 (1)	0.19654 (4)	2.79 (2)
S1	−0.02073 (9)	0.0359 (3)	0.1740 (1)	3.4 (1)
S2	−0.0563 (1)	−0.2515 (3)	0.2782 (1)	4.0 (1)
S3	−0.15818 (9)	−0.1624 (4)	0.2293 (1)	4.4 (1)
P	−0.12203 (9)	0.0240 (3)	0.1184 (1)	3.0 (1)
O1	−0.0592 (3)	−0.3574 (9)	0.1154 (4)	5.7 (3)
N	−0.1110 (3)	0.049 (1)	0.2685 (4)	3.9 (3)
C1	−0.0700 (4)	−0.260 (1)	0.1449 (4)	4.4 (3)
C2	−0.1493 (4)	−0.012 (2)	0.1449 (5)	4.2 (3)
C11	−0.0933 (5)	0.161 (1)	0.3074 (5)	4.8 (3)
C12	−0.1107 (7)	0.169 (2)	0.3686 (6)	9.0 (6)
C13	−0.0441 (6)	0.377 (2)	0.3286 (8)	8.6 (6)
C14	−0.060 (1)	0.379 (2)	0.3888 (9)	12.9 (10)
C15	−0.094 (1)	0.279 (2)	0.4059 (8)	12.8 (10)
C16	−0.0623 (4)	0.263 (1)	0.2892 (6)	4.9 (4)
C21	−0.1585 (3)	−0.097 (2)	0.0721 (5)	4.4 (3)
C22	−0.1646 (4)	−0.256 (2)	0.0853 (6)	4.7 (3)
C23	−0.1915 (5)	−0.338 (2)	0.0482 (6)	5.7 (4)
C24	−0.2126 (5)	−0.271 (2)	−0.0011 (7)	6.3 (4)
C25	−0.2050 (4)	−0.118 (2)	−0.0129 (7)	6.2 (4)
C26	−0.1789 (4)	−0.029 (2)	0.0212 (5)	4.7 (4)
C31	−0.0884 (4)	0.115 (2)	0.0588 (4)	4.5 (3)
C32	−0.0807 (5)	0.272 (2)	0.0566 (7)	7.2 (5)
C33	−0.0537 (7)	0.329 (2)	0.0113 (8)	9.8 (7)
C34	−0.0381 (5)	0.229 (2)	−0.0344 (7)	7.4 (5)
C35	−0.0434 (5)	0.074 (2)	−0.0300 (6)	7.5 (6)
C36	−0.0692 (4)	0.015 (2)	0.0171 (6)	5.9 (4)
C41	−0.1555 (3)	0.181 (1)	0.1451 (4)	3.6 (3)
C42	−0.2020 (4)	0.183 (1)	0.1384 (6)	5.0 (4)
C43	−0.2254 (4)	0.301 (2)	0.1625 (7)	6.5 (5)
C44	−0.2057 (5)	0.421 (2)	0.1929 (6)	6.2 (4)
C45	−0.1600 (4)	0.422 (2)	0.0212 (5)	5.0 (4)
C46	−0.1360 (4)	0.299 (1)	0.1749 (5)	4.3 (3)
OA1	0.2924 (5)	0.330 (2)	0.1061 (7)	11.1 (5)
CA1	0.3061 (9)	0.207 (2)	0.122 (1)	12.5 (9)
CA2	0.2729 (7)	0.117 (3)	0.1600 (8)	12.2 (8)
CA3	0.3478 (8)	0.142 (3)	0.104 (1)	12.7 (9)

(s), 716 (s), 754 (m), 916 (w), 1104 (s) cm^{-1}. FABMS: m/e 1148 (M + H$^+$), 1067 (M$^+$ − C_5H_5N), 990 (M$^+$ − $2C_5H_5N$), 962 (M$^+$ − CO − $2C_5H_5N$), 933 (M$^+$ − C_5H_5N − PhNCHS), 857 (M$^+$ − $2C_5H_5N$ − PhNCHS), 825 (M$^+$ − CO − $2C_5H_5N$ − PhNCHS). ^{1}H NMR: S–CH–N, δ 9.91 (s), 8.48 (d), $^4J_{P-H}$ = 2.44 Hz; py H α, δ 8.29 (d), $^3J_{H-H}$ = 4.88 Hz, δ 8.18 (d), $^3J_{H-H}$ = 5.38; δ 6.34, 7.85 (m).

Compound **11** was also isolated by irradiating a solution of **1** (0.13 g, 1 × 10^{-4} mol) in 200 mL of pyridine (py) for 10 min. The reaction solution was concentrated to 5 mL under reduced pressure, and then an excess of 2-propanol and *n*-hexane was added to precipitate green powder. The precipitate was purified on a neutral Al_2O_3 TLC plate with benzene as eluent. The yield was about 8%.

Table IV. Positional and Thermal Parameters for $[(PhNCHS)Ru(CO)(PPh_3)]_2(WS_4)\cdot 2C_3H_6O$

atom	x/a	y/b	z/c	B, Å^2
W	0.0	−0.1124 (1)	0.25	2.87 (2)
Ru	−0.08514 (5)	−0.1047 (2)	0.19625 (7)	2.68 (3)
S1	−0.0207 (1)	0.0333 (6)	0.1740 (2)	3.1 (1)
S2	−0.0559 (2)	−0.2545 (6)	0.2780 (3)	3.7 (1)
S3	−0.1577 (2)	−0.1663 (7)	0.2291 (3)	4.0 (1)
P	−0.1220 (2)	0.0203 (6)	0.1183 (2)	2.8 (1)
O1	−0.0593 (5)	−0.361 (2)	0.1151 (8)	6.3 (5)
N	−0.1154 (5)	0.048 (2)	0.2677 (7)	3.1 (4)
C1	−0.0694 (7)	−0.263 (2)	0.1443 (9)	3.7 (6)
C2	−0.1486 (8)	−0.015 (3)	0.276 (1)	5.1 (7)
C11	−0.0939 (7)	0.159 (2)	0.309 (1)	4.2 (6)
C12	−0.110 (1)	0.171 (3)	0.368 (1)	7.2 (10)
C13	−0.0444 (8)	0.363 (3)	0.330 (1)	9.2 (13)
C14	−0.0595 (1)	0.372 (3)	0.391 (2)	10.2 (13)
C15	−0.0935 (1)	0.277 (4)	0.406 (1)	7.1 (9)
C16	−0.0627 (7)	0.266 (2)	0.289 (1)	4.8 (7)
C21	−0.1560 (6)	−0.101 (3)	0.0721 (9)	4.1 (6)
C22	−0.1640 (7)	−0.258 (3)	0.086 (1)	7.3 (10)
C23	−0.1916 (7)	−0.348 (3)	0.048 (1)	8.3 (11)
C24	−0.2125 (8)	−0.282 (3)	−0.002 (1)	7.7 (10)
C25	−0.2047 (8)	−0.123 (3)	−0.014 (1)	7.1 (9)
C26	−0.1765 (6)	−0.038 (3)	0.021 (1)	5.9 (8)
C31	−0.0885 (6)	0.110 (3)	0.0600 (9)	3.9 (6)
C32	−0.081 (1)	0.268 (3)	0.058 (1)	4.5 (6)
C33	−0.052 (1)	0.324 (3)	0.011 (1)	4.6 (7)
C34	−0.0372 (9)	0.223 (4)	−0.035 (1)	5.5 (8)
C35	−0.0457 (9)	0.074 (4)	−0.030 (1)	5.3 (7)
C36	−0.0686 (8)	0.018 (3)	0.018 (1)	4.5 (7)
C41	−0.1566 (6)	0.175 (2)	0.1452 (8)	2.8 (5)
C42	−0.2018 (7)	0.175 (3)	0.138 (1)	4.6 (6)
C43	−0.2284 (7)	0.291 (3)	0.162 (1)	5.3 (8)
C44	−0.2069 (9)	0.412 (3)	0.195 (1)	6.2 (8)
C45	−0.1632 (8)	0.416 (3)	0.0200 (9)	5.3 (7)
C46	−0.1367 (6)	0.295 (2)	0.1763 (9)	3.4 (5)
OA1	0.2921 (8)	0.330 (3)	0.106 (1)	10.7 (9)
CA1	0.306 (1)	0.207 (4)	0.122 (2)	8.5 (11)
CA2	0.273 (2)	0.116 (7)	0.160 (2)	18.7 (24)
CA3	0.348 (1)	0.141 (6)	0.105 (2)	16.1 (20)

Collection and Reduction of X-ray Data. Crystals of **3** and its Mo analogue were subjected to single-crystal X-ray diffraction analysis. Unit cell parameters were obtained from a least-squares fit of 20 reflections in the range 20° < 2θ < 25° measured on a Rigaku AFC-5R four-circle diffractometer using graphite-monochromated Mo Kα radiation. The details of the data collections are given in Tables I and II and in supplementary Tables S1 and S2. Since the crystals were not stable against X-ray irradiation, crystals coated with epoxy resin were used for measurements.

Solution and Refinement of the Structures. The coordinates of the metal atoms were found by direct method, and a series of block-diagonal least-squares refinements followed by Fourier synthesis revealed all the remaining atoms except hydrogen atoms. The structure was finally refined with anisotropic temperature factors for all the atoms to the final discrepancy index of R = 0.065 and R_w = 0.072 for **1** and R = 0.080 and R_w = 0.090 for **3**, where $R = \sum||F_o| - |F_c||/\sum|F_o|$ and $R_w = [\sum w_i(|F_o| - |F_c|)^2/\sum w_i|F_o|^2]^{1/2}$ ($w_i = (1/\sigma^2(F))$). Atomic scattering factors and anomalous dispersion corrections were taken from ref 19. All the calculations were performed with the program systems UNICS-III[20] and ORTEP.[21] Absorption correction was made for **3** by following the method of North et al.[22] Absorption correction was not applied to **1**, since its absorption coefficient is small. No extinction correction was made for both crystals. The hydrogen atoms were introduced at their calculated positions (C–H fixed at 1.09 Å) with isotropic thermal parameters. Since both crystals were not stable against X-ray irradiation, diffraction intensities were corrected according to the intensity changes of the standard reflections and were used for calculation. However, the final R values were not sufficiently low due to the deterioration of the crystals. The standard intensities decreased to 92% finally on an average.

(19) *International Tables for X-ray Crystallography*; Kynoch Press: Birmingham, England, 1974; Vol. IV, pp 99, 149.
(20) Sakurai, T.; Kobayashi, K. *Rigaku Kenkyusho Hokoku* **1979**, *55*, 69.
(21) Johnson, C. K. Report ORNL-3794 (revised); Oak Ridge National Laboratory: Oak Ridge, TN, 1976.
(22) North, A. T. C.; Philips, D. C.; Mathews, F. S. *Acta Crystallogr.* **1968**, *A24*, 351.

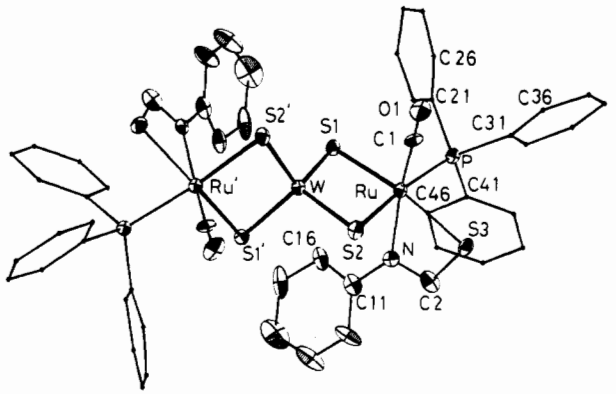

Figure 1. Molecular structure of $[(PhNCHS)Ru(CO)(PPh_3)]_2(WS_4)\cdot 2(CH_3)_2CO$ (**3**). Carbon atoms of PPh_3 are drawn artificially small for clarity. The carbon atoms in the phenyl rings are numbered consecutively according to their positions in each ring, e.g., C*n*1–C*n*6 (*n* = 1–4). The thermal ellipsoids are drawn at 30% probability.

Table V. Interatomic Distances (Å) for $[(PhNCHS)Ru(CO)(PPh_3)]_2(MoS_4)\cdot 2C_3H_6O$

	Metal–Metal		
Mo–Ru	2.8646 (8)		
	Coordination Bond		
Mo–S1	2.215 (3)	Mo–S2	2.217 (3)
Ru–S1	2.364 (3)	Ru–S2	2.404 (3)
Ru–S3	2.423 (3)	Ru–P	2.359 (3)
Ru–N	2.227 (9)	Ru–C1	1.85 (1)
	Ligand Geometry		
C1–O1	1.12 (1)	C2–N	1.30 (2)
S3–C2	1.69 (1)	P–C21	1.86 (1)
P–C31	1.86 (1)	P–C41	1.81 (1)
N–C11	1.42 (2)		

The final positional and thermal parameters for **1** are listed in Table III. Those for **3** are listed in Table IV. The anisotropic temperature factors for **1** (Table S3) and **3** (Table S4), the observed and calculated structure factors (Tables S5 and S6 for **1** and **3**, respectively), and the final positional and thermal parameter for **1** and **3** (Tables S7 and S8) are available as supplementary materials.

Physical Measurements. Infrared spectra were recorded on a Perkin-Elmer FTIR 1640 instrument, and UV–vis spectra were measured on a Shimadzu UV-260 spectrophotometer. $^{31}P\{^1H\}$ NMR spectra were recorded on a JEOL 90A instrument, whereas ^1H and ^{13}C NMR spectra were measured on a JEOL FX400 instrument by using $CDCl_3$ as solvent. The chemical shifts are expressed in ppm, which is referenced to an external standard of 85% H_3PO_4 for ^{31}P and TMS for ^1H and ^{13}C. Resonance Raman spectra were measured on a Spex Ramlog 6 double monochromator. The excitation source was the 514.5-nm line from an Ar^+ laser. FAB mass spectra were obtained on a JEOL JMS-HX110 instrument. The samples were measured as nitrobenzyl alcohol solutions.

Results

Structure of the Complexes. The structure of complex **3** with the atomic numbering scheme is shown in Figure 1. Since the crystals of **1** and **3** are isomorphous and the crystal and molecular differences in bond distances and angles are small, the following description is mainly concerned with **3**, since crystal structures of similar Ru–M–Ru trinuclear compounds with sulfur bridges have been reported only for M = W. The description of **1** is limited to areas where the comparison of the two structures is significant and chemically important.

Molecule **3** has C_2 symmetry, and the central tungsten atom is located crystallographically on a 2-fold axis along the *b* axis and on a diagonal glide plane. The tungsten atom is tetrahedrally coordinated by four sulfur atoms, and two of them coordinate to a ruthenium atom in the cis position. The ruthenium atom completes octahedral coordination, being coordinated further by sulfur and nitrogen atoms of a PhNCHS chelate and CO and PPh_3. Selected bond distances for **1** and **3** are presented in Tables V and VI, respectively. All the bond lengths for **1** (Table S9) and **3** (Table S10) and the bond angles for **1** (Table S11) and **3** (Table S12) are deposited.

Table VI. Interatomic Distances (Å) for $[(PhNCHS)Ru(CO)(PPh_3)]_2(WS_4)\cdot 2C_3H_6O$

	Metal–Metal		
W–Ru	2.886 (2)		
	Coordination Bond		
W–S1	2.213 (5)	W–S2	2.213 (6)
Ru–S1	2.375 (5)	Ru–S2	2.411 (4)
Ru–S3	2.415 (6)	Ru–P	2.347 (5)
Ru–N	2.21 (1)	Ru–C1	1.87 (2)
	Ligand Geometry		
C1–O1	1.12 (2)	C2–N	1.29 (3)
S3–C2	1.73 (2)	P–C21	1.82 (2)
P–C31	1.82 (2)	P–C41	1.82 (2)
N–C11	1.44 (2)		

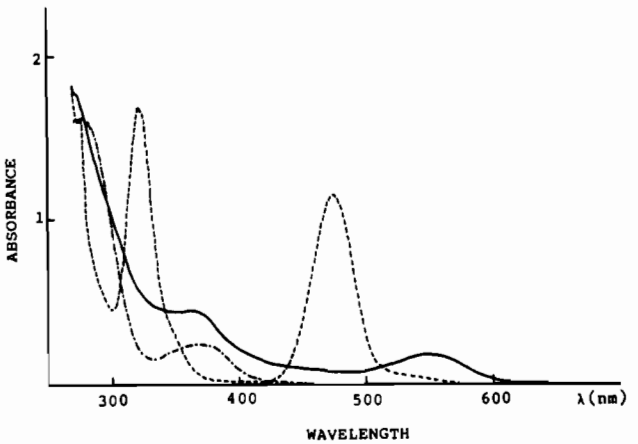

Figure 2. UV–vis spectra in DMF: (—) [**1**] = 2.67×10^{-5} M; (---) $[(PPh_4)_2MoS_4] = 8.11 \times 10^{-5}$ M; (-·-) $[RuCl(PhNCHS)(CO)(PPh_3)_2] = 4.36 \times 10^{-5}$ M.

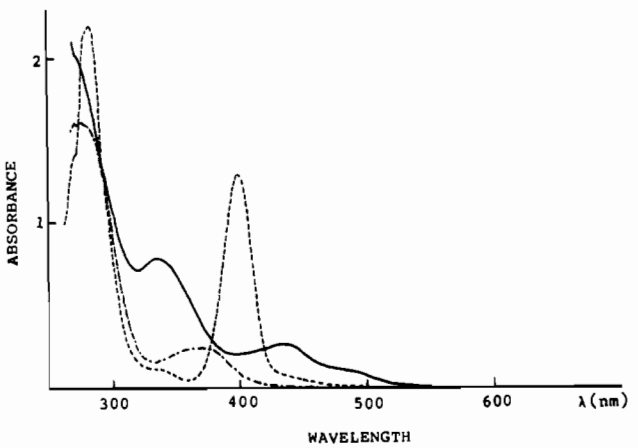

Figure 3. UV–vis spectra in DMF: (—) [**2**] = 2.60×10^{-5} M; (---) $[(PPh_4)_2WS_4] = 6.98 \times 10^{-5}$ M; (-·-) $[RuCl(PhNCHS)(CO)(PPh_3)_2] = 4.36 \times 10^{-5}$ M.

Synthesis and Spectroscopic Properties. Trimetallic compounds of the formula $[(L)Ru(CO)(PPh_3)]_2MS_4$ are readily prepared from the reaction of 2 equiv of $RuCl(L)(CO)(PPh_3)_2$ with $(Ph_4P)_2MS_4$ as shown in eq 1. The resulting trinuclear compounds

$$2RuCl(L)(CO)(PPh_3)_2 + (Ph_4P)_2MS_4 \rightarrow [(L)Ru(CO)(PPh_3)]_2MS_4 + 2PPh_3 \quad (1)$$

$$M = Mo, W$$

are air stable and have been characterized by spectroscopic methods. The summary of various spectroscopic data is shown in Table VII. The spectroscopic properties of the starting materials are summarized in Table VIII for comparison. The UV–vis spectra of **1** and **2** are shown in Figures 2 and 3, respectively. Those of **4**–**7** are basically the same as those in Figures 2 and 3

Table VII. Spectroscopic Data for $Ru(\mu\text{-}MS_4)Ru$ (M = Mo, W) Trinuclear Complexes

complex	IR,[a] cm^{-1} ν(M–S)	IR,[a] cm^{-1} ν(C–O)	RR, cm^{-1} ν(M–S)	UV–vis[e] λ_{max}, nm (ϵ, M/cm)	$^{31}P\{^1H\}$ NMR[f] δ, ppm
$[(PhNCHS)Ru(CO)(PPh_3)]_2(MoS_4)$ (**1**) red	462, 424	1973	439, 475[a,b]	363.4 (1.7×10^4) 552.2 (6.7×10^3)	42.20 (s)
$[(PhNCHS)Ru(PPh_3)](MoS_4)[(PPh_3)(CO)Ru(PhNCHS)]$ (**10**) green	460, 436	1956	*d*	662.4 (5.0×10^3)	43.07 (s), 42.52 (s) 38.09 (s), 37.10 (s)
$[(PhNCHS)Ru(C_5H_5N)_2](MoS_4)[(PPh_3)(CO)Ru(PhNCHS)]$ (**11**) green	460, 430	1956	*d*	365.8 (2.2×10^4) 699.0 (7.0×10^3)	43.54 (s)
$[(PhNCHS)Ru(C_5H_5N)_2]_2(MoS_4)$ (**8**) brown	456		*d*	364.6 (1.6×10^4) 405.4 (1.4×10^4) 752.0 (6.5×10^3)	
$[(PhNCHS)Ru(CO)(PPh_3)]_2(WS_4)$ (**2**) orange	447	1977	*d*	350.0 (3.1×10^4) 436.0 (1.0×10^4)	41.87 (s)
$[(PhNCHS)Ru(C_5H_5N)_2]_2(WS_4)$ (**9**) green	442		454[a,c]	354.4 (1.3×10^4) 405.8 (1.9×10^4) 594.8 (1.0×10^4)	
$[\{C_2H_4(C_5H_4N)\}Ru(CO)(PPh_3)]_2(MoS_4)$ (**4**) red	459, 436	1940	438, 875[b,e]	354.8 (1.7×10^4) 559.8 (1.0×10^3)	52.97 (s)
$[\{C_2H_4(C_5H_4N)\}Ru(CO)(PPh_3)]_2(WS_4)$ (**5**) yellow	448	1936	*d*	337.8 (1.6×10^4) 467.6 (6.8×10^3)	53.04 (s)
$[\{C_2H_4C(O)OMe\}Ru(CO)(PPh_3)]_2(MoS_4)$ (**6**) red	459, 430	1945	436, 871[b,e]	344.0 (1.8×10^4) 548.0 (8.9×10^3)	50.48 (s)
$[\{C_2H_4C(O)OMe\}Ru(CO)(PPh_3)]_2(WS_4)$ (**7**) yellow	448	1944	*d*	304.4 (2.6×10^4) 458.2 (7.3×10^3)	50.78 (s)

[a] KBr pellet. [b] λ_e = 514.5 nm. [c] λ_e = 568.2 nm. [d] Could not be obtained. [e] CH_2Cl_2 solution. [f] $CDCl_3$ solution, referenced to H_3PO_4. All spectra are proton decoupled.

Table VIII. Spectroscopic Data for the Starting Materials

complex	IR,[a] cm^{-1} ν(M–S)	IR,[a] cm^{-1} ν(C–O)	UV–vis[b] λ_{max}, nm (ϵ, M/cm)	$^{31}P\{^1H\}$ NMR[c] δ, ppm
$RuCl(PhNCHS)(CO)(PPh_3)_2$		1923, 1944	378.2 (5.7×10^3)	35.00 (s)
$RuCl\{CH_2CH_2(C_5H_4N)\}(CO)(PPh_3)_2$		1905		40.95 (s)
$RuCl\{CH_2CH_2C(O)OMe\}(CO)(PPh_3)_2$		1905		39.42 (s)
$(Ph_4P)_2MoS_4$	469		323.2 (2.6×10^4) 476.2 (1.8×10^4)	
$(Ph_4P)_2WS_4$	449		282.8 (2.7×10^4) 400.2 (1.9×10^4)	

[a] KBr pellet. [b] DMF solution. [c] $CDCl_3$ solution, referenced to H_3PO_4. All spectra are proton decoupled.

and the λ_{max}'s are shown in Table VII. The spectra of compounds **8–11** are shown in Figure 4.

Discussion

Structure of the Complexes. The structure of the bis(acetone) adduct of complex **2** (**3**) is shown in Figure 1. One of the PPh_3 ligands and chloride ion have been replaced by the two sulfur atoms of the MS_4^{2-} group. The P atom of PPh_3 and the sulfur atom of PhNCHS are trans to the sulfur atoms of the coordinated MS_4^{2-} group. The W–S distances (2.213 (5) Å on an average) are comparable to those in $Cp_2Ru_2(MeNC)_2WS_4$ (2.212 (6) Å),[13] and $[(Ru(bpy)_2)_2WS_4]^{2+}$ (2.218 (2) Å)[14] but are longer than those in $(NH_4)WS_4$ (2.165 Å).[23] Since there is no previous report on the structures of trimetallic $Ru\text{–}MoS_4\text{–}Ru$ compounds, it is impossible to compare the Mo–S distance in the present compounds with those in other analogous $Ru\text{–}MoS_4\text{–}Ru$ compounds; however, the Mo–S distance (2.21 (3) Å on an average) in **1** is significantly longer than those in $(NH_4)_2MoS_4$ (2.178 (5) Å).[27] The relatively short Mo–Ru and W–Ru distances of 2.8646 (8) and 2.886 (2) Å and the acute Ru–S–Mo and Ru–S–W angles of 77.4 (1) and 76.5 (1)° for M = Mo and 77.7 (2) and 77.1 (1)° for M = W indicate metal–metal bondings as reported previously for other trimetallic $Ru\text{–}(MS_4)\text{–}Ru$ complexes. The metal–metal bond

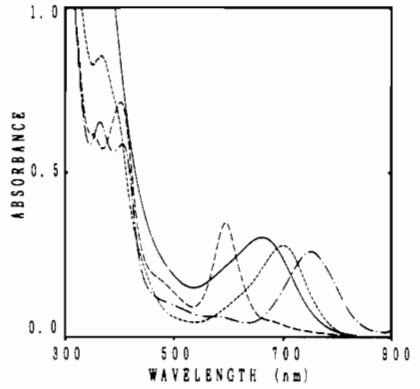

Figure 4. UV–vis spectra of **8–11** in CH_2Cl_2: (—) [**10**] = 4.5×10^{-5} M; (···) [**11**] = 4.0×10^{-5} M; (–·–) [**8**] = 4.0×10^{-5} M; (- - -) [**9**] = 2.5×10^{-5} M.

distances and angles are slightly larger than those in $Cp_2Ru_2(MeNC)_2WS_4$ (W–Ru = 2.870 (2) Å and Ru–S–W = 77.0 (2) and 77.3 (2)°)[13] and $[(Ru(bpy)_2)_2WS_4]^{2+}$ (W–Ru = 2.838 (1) Å and Ru–S–W = 76.2 (1) and 76.6 (1)°).[14] The latter complex seems to have the strongest metal–metal bonding, as seen from its W–Ru distance, among trinuclear Ru–W–Ru complexes of this sort. Coordination of the π-acceptor ligands like CO or PPh_3 to Ru probably decreases π-back-donation from Ru to other ligands, thus increasing the Ru–S distances for the bridging S atoms. The Ru–S distances in compound **2** are 2.375 (5) and 2.411 (4) Å. In comparison, the Ru–S bond in the S-bound thiophene complex $[(C_5H_4CH_2\text{-}2\text{-}C_4H_3S)Ru(PPh_3)_2](BF_4)^{24}$ is 2.41 Å, whereas those in $[(Ru(bpy)_2)_2WS_4]^{2+}$ are 2.376 (2) and 2.369 (3) Å[14] and the Ru–S bonds are 2.394 (6) and 2.377 (6)

(23) Sasvari, K. *Acta Crystallogr.* **1963**, *16*, 719.
(24) Draganjac, M. E.; Rauchfuss, T. B.; Ruffing, C. J.; Wilson, S. R. *Organometallics* **1985**, *4*, 1909.
(25) Ambrosius, H. P. M. M.; Van Hemert, A. W.; Bosman, W. P.; Noordik, J. H.; Ariaans, G. J. A. *Inorg. Chem.* **1984**, *23*, 2678.
(26) (a) Muller, A.; Diemann, E.; Josters, R.; Bogge, H. *Angew. Chem., Int. Ed. Engl.* **1981**, *20*, 934. (b) Muller, A.; Hellmann, W. *Spectrochim. Acta, Part A.* **1985**, *41*, 359.
(27) Lapasset, P. J.; Chezeau, N.; Belougne, P. *Acta Crystallogr.* **1976**, *B32*, 3087.

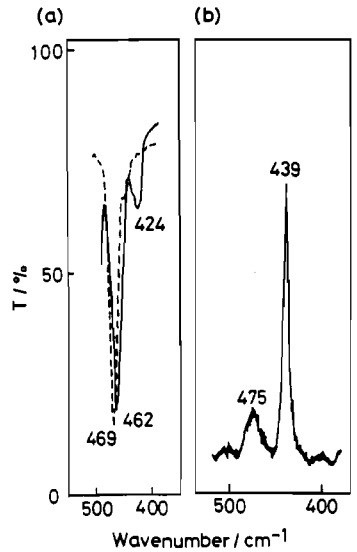

Figure 5. (a) IR spectra for complex **1** (—) and $(Ph_4P)_4MoS_4$ (---). (b) Resonance Raman spectrum of complex **1**. Excitation wavelength: 514.5 nm. All spectra were obtained as KBr pellet samples.

Å in $Cp_2Ru_2(MeNC)_2WS_4$.[13] The difference of the two Ru–S distances in Ru–S1 (2.375 (5) Å) and Ru–S2 (2.411 (4) Å) in compound **2** would be a result of the difference of the trans influence of PPh_3 (trans to S2) and a sulfur atom of PhNCHS (trans to S1). The structures of the two compounds **1** and **2** are basically very similar to each other. The difference in their bond distances are that (1) both Ru–S1 and Ru–S2 are longer in the Ru–WS_4–Ru compound **2** than in the Ru–MoS_4–Ru compound, (2) Ru···M distances are longer for M = W than for M = Mo. (3) Ru–P, Ru–S3, and Ru–N distances are longer for the Ru–MoS_4–Ru compound **1** than those for the Ru–WS_4–Ru compound **2**. These facts suggest that π-back-donation from Ru to MS_4 is stronger for M = Mo than for M = W. This tendency has been reported for other trimetallic compounds: for example, $(PPh_4)_2[FeCl_2)_2(MoS_4)]$, Fe–Mo = 2.775 Å, Fe–S = 2.204 Å; $(PPh_4)_2[(FeCl_2)_2(WS_4)]$, Fe–W = 2.801 Å, Fe–S = 2.209 Å.[26] The ligand geometries are normal and the geometry of NCS in the PhNCHS chelate is comparable to that in $Mo(CO)_2(\eta^5$-$C_5H_5)[Ph_2P(S)CSNPh]$ (N–C = 1.321 (5) Å, C–S = 1.709 (7) Å, N–C–S = 110.4°).[25]

Spectroscopic Properties. In all trimetallic compounds the ν(CO)'s are shifted 30–40 cm^{-1} to higher wavenumbers compared to those of the starting Ru compounds (see Tables VII and VIII). This fact suggests that MS_4^{2-} has stronger π-acceptor nature compared to Cl^- or PPh_3, and coordination of MS_4^{2-} to Ru has the effect of weakening the Ru–CO bond. This renders the trinuclear compound substitutionally more labile at the CO ligand than the starting mononuclear Ru compound. In comparison of the three chelate ligands, compounds **1** and **2** show higher ν(CO), compared to those with other chelate ligands, indicating that the π-accepting nature of PhNCHS is stronger and CO is more weakly coordinated in **1** and **2**, compared to the trimetallic compounds with other two chelate ligands.

The IR and resonance Raman spectra of **1** are shown in Figure 5. All the bands are assigned to ν(Mo–S) stretching vibrations.[26] Two ν(Mo–S) bands are observed for **1**, whereas free MoS_4^{2-} has only one band in this region. This difference is due to the distortion of the MoS_4^{2-} tetrahedron in the trinuclear complex **1** from T_d symmetry, and the originally IR-inactive vibrational mode has become active. The trimetallic complex formation weakens the Mo–S bonds and therefore the ν(Mo–S) is shifted to lower wavenumbers in **1** compared to that of free MoS_4^{2-}. Characteristic band shifts due to complex formation are also observed in UV–vis spectra in the range 340–370 and 550–560 nm (M = Mo) and 300–350 and 430–460 nm (M = W) (Figures 2 and 3). Similar absorptions are also found in $[Cp(PPh_3)Ru]_2MS_4$[13] and $[(Ru(bpy)_2)_2MS_4](PF_6)_2$.[14] The assignment of the bands in Figures 2 and 3 is supported by the enhancement of the resonance Raman intensity of **1** by the excitation with λ_e = 514.5 nm as shown in Figure 5. Muller and co-workers have also reported in their resonance Raman study of thiometalate complexes $M'S_2MS_2$ and $M'S_2MS_2M'$ (M = Mo, W; M' is the other transition elements) that excitation at around 500 nm resulted in enhanced ν(Mo–S) bands.[26] In the present study the absorption band (λ = 476 nm, LMCT of S–Mo) of MoS_4^{2-} is shifted to a longer wavelength by complex formation. These results show that the bands in the range 550–560 nm (M = Mo) are assigned to LMCT of S–Mo. The complexes **1**, **4**, and **6** show ν(M–S) in the range 430–480 cm^{-1} in their resonance Raman spectra. In the spectra of **4** and **6**, second-order vibrations were also observed at 875 and 871 cm^{-1}, respectively. The corresponding bands were not detected for the analogous tungsten complexes **2**, **5**, and **7**, since the resonance bands of these complexes are in the UV region (ca. 400 nm) and irradiation in the UV region resulted in decomposition of the compounds. The photochemical decomposition is related to the photochemical ligand elimination and substitution reactions of these compounds, and more details will be described in the following sections.

On trimetallic complex formation, an electron is redistributed from the Ru to the bridging sulfur atoms or further to the central M atom (M = Mo, W), which is indicated by ν(CO) band shifts on complex formation. The electron redistribution from Ru to the bridging MS_4 group is also manifested in $^{31}P\{^1H\}$ NMR spectra. Since the electron redistribution throughout the Ru–MS_4–Ru framework decreases the electron density at the Ru atoms and also the magnetic shield at the P atoms of the PPh_3 ligands, ^{31}P chemical shifts for trinuclear complexes are shifted to lower field than those for the starting mononuclear ruthenium complexes. Mössbauer spectroscopy,[3] electronic spectroscopy,[3] resonance Raman spectroscopy,[26] IR spectroscopy,[26] and theoretical study[28,29] of $M'S_2MS_2$ all indicates that the electron redistribution in M'–MS_4^{2-} is not limited only to M'–S bondings but is further extended to the entire binuclear structure. The present ν(C–O) bands and $^{31}P\{^1H\}$ NMR spectra also conform to the delocalized electronic state in the Ru–MS_4–Ru structure.

Each of the symmetric trinuclear complexes shows only one ^{31}P signal, which indicates the equivalence of the two Ru atoms on both sides of the MS_4 group. The ^{13}C NMR spectrum of **1** shows peaks at 180.8 ppm (CO), with $^2J_{C-P}$ = 35.2 Hz, and 144.7 ppm (S–C–N), with $^3J_{C-P}$ = 11.0 Hz, which also proves the equivalence of the two Ru atoms.

Ligand Substitution and Elimination Reactions. Complexes **1** and **2** undergo a variety of chemical and photochemical ligand substitution and elimination reactions. For example, irradiation of a pyridine solution of **1** with a high-pressure mercury lamp afforded **8** and **11** as eqs 2 and 3 show, where both CO and PPh_3

$$[(PhNCHS)Ru(CO)(PPh_3)]_2MS_4 \xrightarrow[\text{pyridine}]{h\nu} [(PhNCHS)Ru(py)_2](\mu\text{-}MS_4)[(PPh_3)(CO)Ru(PhNCHS)] \quad (2)$$

$$[(PhNCHS)Ru(CO)(PPh_3)]_2(MS_4) \xrightarrow[\text{pyridine}]{h\nu} [(PhNCHS)Ru(py)_2]_2MS_4 \quad (3)$$

M = Mo, W

are substituted by py. Although photochemical substitution reactions of CO in mononuclear or binuclear metal–carbonyl compounds and photolytic cleavage reactions of multinuclear metal–carbonyl cluster compounds are widely known,[30] reactions 2

(28) He, L.-J.; Zhang, L.-N.; Lu, J.-X. *Huaxie Xiebao* (*Acta Chim. Sin.*) **1987**, *45*, 676.
(29) Liu, C.-W.; Hua, J.-M.; Chen, Z.-D.; Lim, Z.-Y.; Lu, J.-X. *Int. J. Quantum Chem.* **1986**, *29*, 701.
(30) (a) Sellman, D.; Kappler, O.; Knoch, F. *J. Organomet. Chem.* **1989**, *367*, 161. (b) Pope, K.; Wrighton, M. S. *Inorg. Chem.* **1987**, *26*, 2321. (c) Geoffory, G. L.; Epstein, R. A. In *Inorganic and Organometallic Photochemistry*; Advances in Chemistry Series 168; Wrighton, M. S., Ed.; American Chemical Society: Washington, DC, 1978. (d) Chisholm, M. H., Ed. *Reactivity of Metal-Metal Bonds*; ACS Symposium Series 155; American Chemical Society: Washington, DC, 1981.

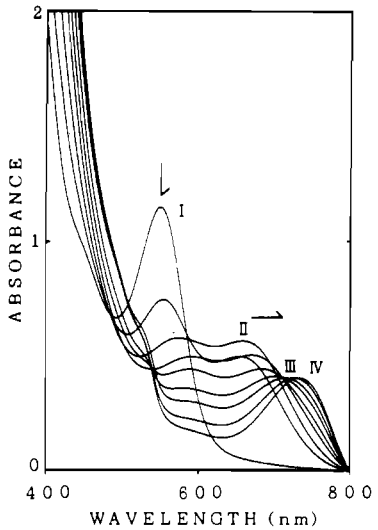

Figure 6. UV–vis spectral changes during reactions 2 and 3 of compound **1** (1.7×10^{-4} M). The spectrum was measured every 2 min.

and 3 depict one of the few examples of photochemical CO substitution in a trinuclear metal compound that is not a metal–carbonyl cluster. Another photochemical substitution of trinuclear compound having a coordinated S atom so far reported is $Fe_3(CO)_9(\mu_2\text{-}H)(\mu_3\text{-}S\text{-}t\text{-}Bu)$, which gives $Fe_3(CO)_8(\eta^2\text{-}\mu_2\text{-}HPhCCPh)(\mu_3\text{-}S\text{-}t\text{-}Bu)$ upon photochemical reaction with PhCCPh.[31] Recently, Rauchfuss et al.[13] reported chemical substitution of PPh_3 by excess CO in a similar MS_4^{2-}-bridged trinuclear compound $[CpRu(PPh_3)]_2WS_4$, where addition of excess CO leads to the formation of $[CpRu(CO)](WS_4)[(PPh_3)RuCp]$. Only one of the PPh_3 groups is substituted in the reaction, and the monocarbonyl product resists further carbonylation. Treatment of a solution of $[CpRu(PPh_3)]_2WS_4$ with PMe_3, MeNC, *t*-BuNC, or benzyl isocyanide, on the other hand, leads to the isolation of disubstituted products $(CpRuL)_2WS_4$ (L = PMe_3, MeNC, *t*-BuNC, benzyl isocyanide).[13] If reactions 2 and 3 are carried out for more than 30 min only decomposition of the product occurs for both M = Mo and W. Reactions 2 and 3 proceed for compound **1** with a color change from red to green and finally to brown as shown in Figure 6. These color changes correspond to the formation of an intermediate **11** and the final product **8**, respectively. The assignment of the intermediate as **11** is based on the comparison of the spectrum with that of isolated compound **11** and also on the fact that a pyridine solution of **11** gives **8** on Hg lamp irradiation. Reactions 2 and 3 for M = W proceed with a color change from yellow (starting material **2**) to red-green and finally to dark green (the final product **9**) as shown in Figure 7. Column chromatography of the reaction solution on neutral Al_2O_3 separated a red component besides dark green **9**. The red component is a reaction intermediate and was confirmed to be a disubstituted trimetallic compound $[(PhNCHS)Ru(py)_2](\mu\text{-}WS_4)[(PPh_3)(CO)Ru(PhNCHS)]$ (**12**), which is a tungsten analogue of **11**, by UV–vis and FAB mass spectrometries. The powder sample obtained by evaporation of the solvent under reduced pressure after a 1-h reaction exhibited major peaks corresponding to **12** at *m/e* 1236 ($M + H^+$), 1156 ($M^+ - C_5H_5N$), 1087 ($M^+ - 2C_5H_5N$) and 1052 ($M^+ - CO - 2C_5H_5N$), although the sample could not be completely purified and elemental analysis did not give a satisfactory result. Reactions 2 and 3 do not occur only by heating the solution of **1** or **2** in py without light. For the photochemical reaction py is essential, and if the reaction is carried out without py, decomposition of the compound occurs. Heating a benzene solution without py also leads only to decomposition of the trimetallic compound. The CO in the starting mononuclear Ru compound $RuCl(PhNCHS)(CO)(PPh_3)_2$ is not substituted under the similar photochemical conditions.

(31) Fassler, T.; Hnttner, G. *J. Organomet. Chem.* **1989**, *376*, 367.

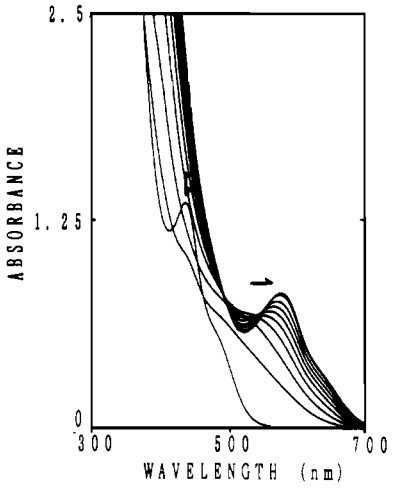

Figure 7. UV–vis spectral change during reactions 2 and 3 of compound **2** (1.4×10^{-4} M). The spectrum was measured every 2 min.

Since coordinated PPh_3 is usually not photochemically dissociated, the first reaction step of reactions 2 and 3 would be a dissociation of CO, which is followed by py substitution. The py coordination promotes the dissociation of PPh_3 and accelerates the second py coordination. This second step is at least partly owing to steric crowding around the Ru atom, since coordinations of bulky PPh_3 and py in a close proximity would sterically be unfavorable.

Similar photochemical substitution reactions were attempted for compounds **4**–**7**; however, these compounds are thermally more unstable than **1** and **2**, and photochemical reaction resulted only in decomposition of the compounds. It should also be remembered that these compounds have their CO groups more tightly bound, as observed in their ν(CO) values, and would need more energy to dissociate their CO ligands.

On the other hand, the coordinated CO in **1** and **2** can be chemically dissociated by treatment of a pyridine solution of **1** or **2** with excess $Me_3NO{\cdot}2H_2O$. The CO dissociation takes place only on one Ru moiety, and even refluxing the pyridine solution does not cause further CO dissociation on the other Ru moiety. Elemental analysis, $^{31}P\{^1H\}$ NMR spectroscopy, and FAB mass spectrometry indicated that the final product has a CO-dissociated five-coordinated Ru atom as shown in eq 4. Although we have

$$[(PhNCHS)Ru(CO)(PPh_3)]_2MS_4 + \text{excess } Me_3NO \xrightarrow[py]{50\ ^\circ C} [(PhNCHS)Ru(PPh_3)](MS_4)[(PPh_3)(CO)Ru(PhNCHS)] \quad (4)$$

M = Mo, W

isolated only the product for M = Mo (compound **10**) and have not isolated the product for M = W, formation of $[(PhNCHS)(PPh_3)Ru](\mu\text{-}WS_4)[Ru(PPh_3)(CO)(PhNCHS)]$ (**13**) as the major product was confirmed by FAB mass spectrometry (*m/e* 1338 ($M - H^+$), 1050 ($M^+ - CO - 2PhNCHS$), 911 ($M^+ - CO - PhNCHS - PPh_3$)). The powder sample of **13** for FAB mass spectrometry was prepared by adding excess *n*-hexane to the reaction solution to precipitate the solid and rinsing the solid with 2-propanol to remove excess Me_3NO. The UV–vis spectral change during reaction 4 for compound **1** is shown in Figure 8, which shows an isosbestic point at 590.0 nm. The spectral change for compound **2** is shown in Figure 9. ^{31}P NMR spectra shown in Figure 10 follow the reaction of **1** and demonstrate that although before the reaction both phosphorus atoms of compound **1** are equivalent (signal at 42.40 ppm), four peaks appear after the reaction has been completed at 43.07, 42.52, 38.09, and 37.10 ppm and the two P atoms of PPh_3 on both Ru atoms of the molecule are not equivalent any longer. It is apparent in Figure 10 that two sets of ^{31}P signals, each of which consists of two peaks, appear as the reaction proceeds. Each set is not a doublet due to a coupling, since the separations of the two peaks in each set are

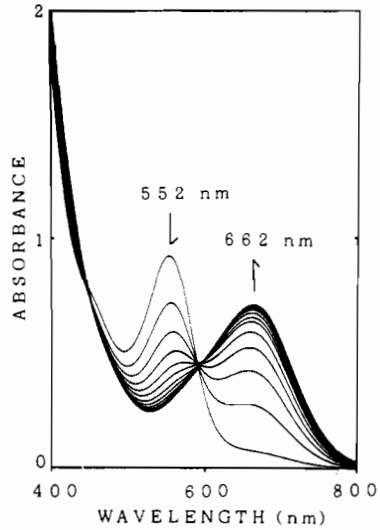

Figure 8. UV–vis spectral change during reaction 4 of compound **1** (1.4×10^{-4} M). The spectrum was measured every 10 min.

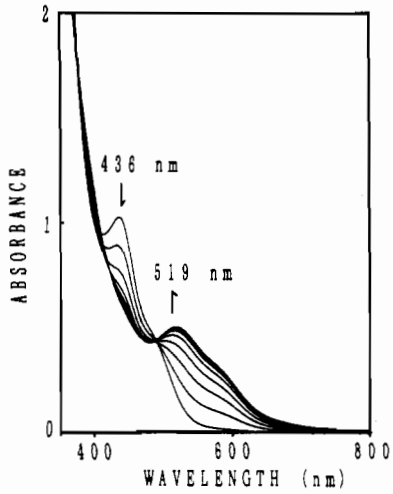

Figure 9. UV–vis spectral change during reaction 4 of compound **2** (1.0×10^{-4} M). The spectrum was measured every 10 min.

different (90.02 and 160.98 Hz). We measured the spectrum of the final solution both at −20 °C and at room temperature, but the relative intensities of the two peaks in each set did not change and the relative intensities of the two sets were equal. The final spectrum is completely the same as that of a solution prepared from a once isolated powder sample of **10**. We also measured a $^{31}P\{^1H\}$ spectrum of the reaction solution by changing the solvent from py to $CDCl_3$, but no spectral change was observed. From these facts and the results of elemental analysis and other spectroscopic properties, we conclude that reaction 4 gives two geometrical isomers as final products. These isomers do not isomerize in solution at least in the temperature range from −20 °C to room temperature, and the relative formation ratio of the two isomers in reaction 4 is not changed on changing the reaction solvent from py to $CDCl_3$. It is not clear at present what the structural relation of the two isomers is; however, it seems most probable that the conformational arrangement of the five ligands around the Ru atom exists in two different forms, which do not easily isomerize in solution. From the spectroscopic data available at present, the structures of the isomers are however not clear. In order to confirm the existence of the two isomers for compound **10**, ^1H NMR in CD_3Cl was measured and the spectrum is shown in Figure 11. The methine proton for PhNCHS of the five-coordinated Ru atom shows two doublet signals at 9.13 and 9.22 ppm with $^4J_{H-P} = 0.98$ and $^4J_{H-P} = 0.97$ Hz, respectively, and the two doublets are almost of equal intensities. The signal for the other methine proton of PhNCHS in the six-coordination sphere is observed as almost like a triplet at 8.401, 8.407, and 8.413 ppm. This seemingly tripletlike

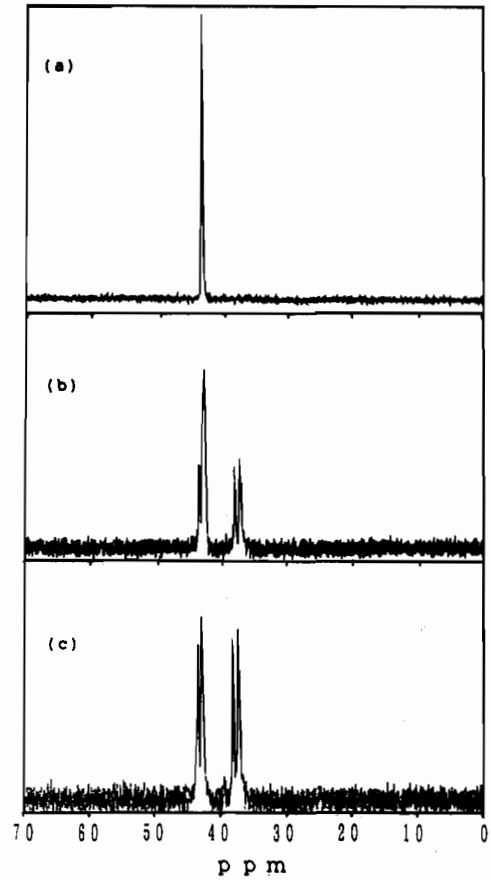

Figure 10. ^{31}P NMR spectra for reaction 4 of compound **1**: (a) before the reaction; (b) during the reaction; (c) after completion of the reaction.

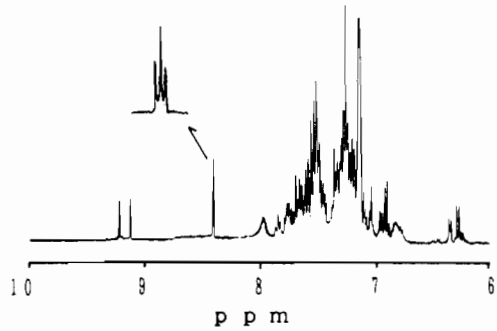

Figure 11. ^1H NMR spectrum of **10** in $CDCl_3$.

signal is actually an overlap of two sets of doublets with almost equal coupling constants, $^4J_{H-P} = 2.44$ Hz. The assignment of these signals to six-coordinated Ru atoms is rationalized by their chemical shifts and $^4J_{H-P}$ values, which are close to those of compounds **1** and **2** having only six-coordinated Ru atoms. The appearances of the two sets of doublets for each methine proton in PhNCHS also rationally explain the existence of two geometrical isomers that differ in the ligand conformation around the five-coordinated Ru atom. We have carefully examined the possible existence of H^- as the sixth ligand by H NMR, but no such hydrogen was detected. There have been several five-coordinated mononuclear Ru complexes reported. The five-coordinated dithiolene complex $[Ru(CO)(PPh_3)_2(S_2C_2(CF_3)_2)]$ should be paid special attention in relevance to the present study, since the complex is reported to exist as two isomers, both of which are square pyramidal, and the orange isomer has axial CO, whereas the violet isomer has axial PPh_3.[32,33] Nothing is mentioned about

(32) Bernal, I.; Clearfield, A.; Ricci, J. S., Jr. *J. Cryst. Mol. Struct.* **1974**, *4*, 43.

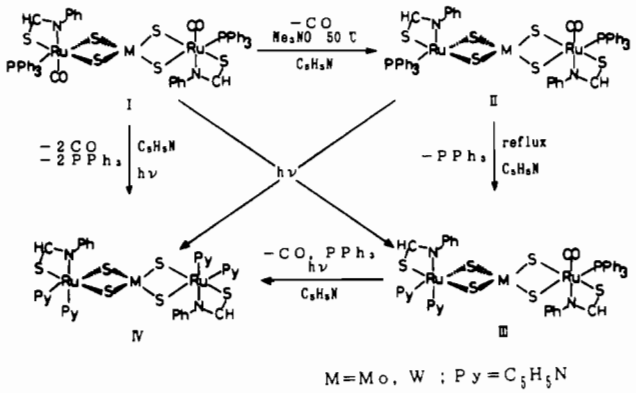

Figure 12. Photochemical and chemical reactions of trimetallic Ru–MS_4–Ru compounds.

the possible existence of agostic hydrogen[34] in these isomers.

Existence of py or pyrazine is essential to reaction 4. It seems that **10** or **13** is stabilized in solution by addition of py. Without py, **10** or **13** is easily decomposed on long standing in either acetone, benzene, or CH_2Cl_2. The stabilization is not due to py coordination, since coordinated py is not observed in ^1H NMR spectroscopy. Similar CO elimination reactions were also attempted for compounds **4**–**7** under the same conditions for **1** and **2**; however, no reaction occurred.

Compounds **10** and **13** undergo ligand addition and substitution as shown in reaction 5, when the pyridine solution is refluxed under

$$[(PhNCHS)Ru(PPh_3)](\mu\text{-}MS_4)[(PPh_3)\text{-}(CO)Ru(PhNCHS)] \xrightarrow[py]{reflux} [(PhNCHS)Ru(py)_2](\mu\text{-}MS_4)[(PPh_3)(CO)Ru(PhNCHS)] \quad (5)$$

M = Mo, W

the conditions described in the Experimental Section. The PPh_3 ligand is substituted by py and the originally five-coordinated Ru atom becomes six-coordinated by py coordination. Reaction 5 leads to decomposition of the complex, if the reaction is carried out in the presence of Me_3NO. This decomposition also occurs even when the reaction temperature is lowered to room temperature. These facts suggest that elimination of the second CO from the six-coordinated Ru atom in compounds **10** or **13** is impossible and the compound is decomposed.

The reaction solution obtained by reaction 5 further undergoes photochemical reaction when the solution is irradiated with a Hg lamp. Final products were confirmed as **8** and **9** by UV–vis spectrometry. It was also confirmed that compound **8** is also obtained by irradiation of the solution from the beginning of reaction 5 without any heating of the solution. The photochemical reactions can be described as follows:

$$[(PhNCHS)Ru(py)_2](\mu\text{-}MS_4)[(PhNCHS)Ru(CO)(PPh_3)] \xrightarrow[py]{h\nu} [(PhNCHS)Ru(py)_2]_2(\mu\text{-}MS_4) \quad (6)$$

$$[(PhNCHS)Ru(PPh_3)](\mu\text{-}MS_4)[(PPh_3)(CO)Ru(PhNCHS)] \xrightarrow[py]{h\nu} [(PhNCHS)Ru(py)_2]_2(\mu\text{-}MS_4) \quad (7)$$

M = Mo, W

From the reaction described so far the whole chemical and photochemical reaction pathways can be drawn as shown in Figure 12. Formations of compounds II and III as intermediates in the photochemical reaction between I and IV are evident in the UV–vis spectra shown in Figure 6.

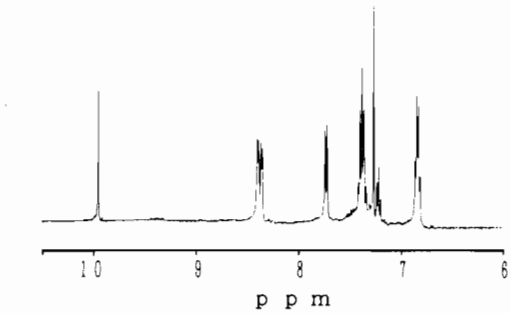

Figure 13. ^1H NMR spectrum of **8** in $CDCl_3$.

We have attempted photosubstitution and chemical-substitution reactions with ligands other than py; however, so far no other ligand has successfully coordinated to the Ru atom. Addition of either N_2H_4, diphenylacetylene, CH_3CN, elemental sulfur, or Et_3N to a benzene solution of **10** did not lead to any reaction even at 50 °C. Heating the solution to refluxing led only to decomposition of the compound. On the other hand, $NOBF_4$ or NO reacted too vigorously even at −70 °C, and the complex was decomposed. We also attempted the photochemical reactions 2 and 3 in the presence of several ligands instead of py and using other solvents. The tested combinations were (i) elemental sulfur and benzene, (ii) N_2H_4 and THF, and (iii) N_2H_4 as both ligand and solvent. All the reactions were carried out at room temperature; however, only decomposition of the complex took place.

Structural Information from NMR Spectroscopy. Although none of the compounds II–IV in Figure 12 have been characterized by single-crystal X-ray analyses, NMR spectroscopy provides information about the ligand geometries around both of the Ru atoms. It seems certain that the coordination geometries of the Ru atoms on the right sides of compounds II and III in Figure 12 are not changed structurally from that of the original compound I, since the $^{31}P\{^1H\}$ signals of II and III which correspond to the PPh_3 ligands on the right side Ru atoms are not shifted considerably from that of compound I as Table VII shows for the molybdenum complexes **1**, **10**, and **11**. It can also safely be stated that the two py ligands in III and IV in Figure 12 are inequivalent and therefore in cis positions, since the two py molecules show clearly two sets of two-line groups in ^1H NMR signals in the range 8–9 ppm, which correspond to two and six H atoms of coordinated py molecules, as shown in Figure 13 for compound **8**. The two py molecules would be equivalent if they are in trans positions. Proton signals of py in this range are due to two and six H atoms (for ^1H NMR assignment, see also the Experimental Section for the synthesis of **8**), and these observations suggest that the two py ligands in these compounds are in cis positions.

Conclusion

The present paper is the first report on the isolation of a sulfur-bridged trinuclear complex which has a coordinatively unsaturated five-coordinated metal site. Although coordination of another ligand to the unsaturated vacant site is successful only with py, and no reaction of the substituted ligand has yet been achieved, the present work is still significant in that it shows a possibility toward photosubstitution of various ligands at cluster complexes that may lead to useful chemical reactions of the coordinated ligand. The failure to introduce other ligands to the vacant coordination site is probably due to the steric blocking of the coordination site by a bulky PPh_3 ligand. Blocking of the sixth coordination site by a very loose interaction of the hydrogen atom of PPh_3 with Ru is proposed in $RuCl_2(PPh_3)_3$.[34] A similar blocking effect of a PPh_3 hydrogen atom is conceivably operating in compound **10**. Heating the reaction solution to accelerate the coordination of the ligand results only in decomposition of the compound. Compound **10** is unstable in O_2, and even slight heating of the solution causes decomposition of the compound. In order to carry out ligand coordination successfully to such coordinatively

(33) Clearfield, A.; Epstein, E. F.; Bernal, I. *J. Coord. Chem.* **1977**, *6*, 227.
(34) *Advanced Inorganic Chemistry*, 5th ed.; Cotton, F. A., Wilkinson, G., Eds.; Wiley Interscience, Inc.: New York, 1988; p 1113.

unsaturated trimetallic compounds, the compound must be thermally more stable or sterically less hindered for the sixth coordination site. Realization of such conditions would be possible by changing or modifying the chelate and PR_3 ligands. The present work is the first demonstration of the possibility for photochemical ligand substitution reactions in sulfur-bridged trimetallic cluster compounds.

Acknowledgment. The present study is financially supported by a Grant-in-Aid for Scientific Research on Priority Area of "Multiplex Organic Systems" (01649008) from the Ministry of Education, Science, and Culture, Japan. Financial support from the Hayashi Memorial Foundation is also gratefully acknowledged.

Supplementary Material Available: Details of the X-ray data collections (Tables S1 and S2), anisotropic temperature factors (Tables S3 and S4), final positional and thermal parameters (Tables S7 and S8), bond lengths (Tables S9 and S10), and bond angles (Tables S11 and S12) (14 pages); observed and calculated structure factors (Tables S5 and S6) (31 pages). Ordering information is given on any current masthead page.

Contribution from the Department of Chemistry and Biochemistry, University of Colorado, Boulder, Colorado 80309

Charge Distribution in Bis(quinone) Complexes of Ruthenium and Osmium. Structural, Spectral, and Electrochemical Properties of the Os(bpy)(Cat)$_2$ (Cat = Catecholate, 3,5-Di-*tert*-butylcatecholate, Tetrachlorocatecholate) Series

Samaresh Bhattacharya and Cortlandt G. Pierpont*

Received June 5, 1991

The series of bis(catecholato)(bipyridine)osmium(IV) complexes have been prepared by treating $Os(bpy)Cl_3$ with either catechol, 3,5-di-*tert*-butylcatechol, or tetrachlorocatechol in the presence of base. Crystals of $Os(bpy)(Cl_4Cat)_2 \cdot 2C_6H_6$ form in the monoclinic crystal system, space group $P2_1/n$, in a unit cell of dimensions $a = 10.906$ (1) Å, $b = 19.395$ (5) Å, $c = 16.953$ (4) Å, $\beta = 91.23$ (1)°, and $V = 3585$ (1) Å^3, for $Z = 4$. The complex molecule is octahedral with chelated bpy and Cl_4Cat ligands. Bond lengths to the metal and C–O lengths of the quinone ligands agree with the bis(catecholato)osmium(IV) charge distribution for the complex in solid state. Electrochemistry and UV–vis–near-IR spectra on the series suggest that in solution the charge distribution is similar to other members of the $M(bpy)(Q)_2$ and $M(PPh_3)_2(Q)_2$ series, with M = Ru, Os and Q = DBQ, Cl_4Q. The five-membered redox series of these complexes show variations in potential with metal, counterligand, and quinone that permit assignment of couples as associated with metal, quinone, or metal–quinone delocalized electronic levels. Metal ion charge appears to remain relatively constant through the series $ML_2(Q)_2^n$, with n ranging from +2 to −2, to the final reduction step which corresponds to a M^{III}/M^{II} reduction. Extreme members of the redox series have well-defined charge distributions as $M^{II}L_2(Cat)_2^{2-}$ and $M^{III}L_2(BQ)(SQ)^{2+}$ species. Neutral forms of the complexes have variable charge distributions in the solid state but have similar properties in solution as delocalized $M^{III}L_2(SQ)(Cat)$ species.

Introduction

Prior to studies on complexes of ruthenium and osmium, the structural, spectral, and magnetic properties of quinone complexes appeared to indicate well-defined charge distributions with metal ions complexed by ligands in either the semiquinone or catecholate forms. This has included many situations where exchange between semiquinone radical ligands and paramagnetic metal ions has resulted in unusual magnetic behavior,[1] where complexes were found to contain mixed-charge semiquinone and catecholate ligands,[2] and cases where the unique bonding properties of these ligands stabilized metal ions in unusual oxidation states.[3] In all cases, localized formal charges could be assigned to the metal ions and to the associated quinone ligands. The work of Lever and Haga has demonstrated that metal–quinone charge delocalization contributes significantly to the electronic structure of the bis(bipyridine)(quinone)ruthenium and -osmium redox series.[4,5] Characterization on the tris(quinone)ruthenium and -osmium complexes has suggested that both metal–quinone delocalization and delocalization between quinone ligands contributes to the electronic structure.[6] In recent studies, we have been interested in the bis(quinone)ruthenium and -osmium complexes, as they offer the opportunity for investigation of both quinone ligand and counterligand effects.[7-9] Counterligands used in these studies have been triphenylphosphine and bipyridine for their different bonding characteristics, quinones have included tetrachloro-1,2-quinone (Cl_4Q), and 3,5-di-*tert*-butyl-1,2-quinone (DBQ), representing ligands with redox potentials that differ by nearly 1 V.[10,11] In the present report, we describe the properties of the $Os(bpy)(Q)_2^n$ redox series, where n varies from +2 to −2 over the five-membered redox series, for the complexes containing DBQ, Cl_4Q, and Q ligands. Results of this study are compared with the properties of the corresponding series of complexes containing either ruthenium or osmium and either PPh_3 or bpy counterligands.[8,9,12]

Experimental Section

Materials. Catechol (H_2Cat), 3,5-di-*tert*-butylcatechol (H_2DBCat), triethylamine, 2,2′-bipyridine, and osmium trichloride hydrate were purchased from Aldrich. Tetrachlorocatechol (H_2Cl_4Cat) was prepared by a published procedure and sublimed before use.[13]

Complex Syntheses. $Os(bpy)Cl_3$. Bipyridine (60 mg, 0.38 mmol) was added to a solution containing 100 mg (0.34 mmol) of $OsCl_3$ in 50 mL of ethanol. A brown solid separated from solution almost immediately.

(1) (a) Buchanan, R. M.; Kessel, S. L.; Downs, H. H.; Pierpont, C. G.; Hendrickson, D. N. *J. Am. Chem. Soc.* **1978**, *100*, 7894. (b) Lynch, M. W.; Buchanan, R. M.; Pierpont, C. G.; Hendrickson, D. N. *Inorg. Chem.* **1981**, *20*, 1038.
(2) (a) Buchanan, R. M.; Pierpont, C. G. *J. Am. Chem. Soc.* **1980**, *102*, 4951. (b) Benelli, C.; Dei, A.; Gatteschi, D.; Pardi, L. *J. Am. Chem. Soc.* **1988**, *110*, 6897. (c) Zakharov, L. N.; Saf'yanov, Yu. N.; Struchkov, Yu. T.; Abakumov, G. A.; Cherkasov, V. K.; Garnov, V. A. *Koord. Khim.* **1990**, *16*, 802.
(3) (a) deLearie, L. A.; Haltiwanger, R. C.; Pierpont, C. G. *Inorg. Chem.* **1987**, *26*, 817. (b) deLearie, L. A.; Pierpont, C. G. *Inorg. Chem.* **1988**, *27*, 3842. (c) deLearie, L. A.; Haltiwanger, R. C.; Pierpont, C. G. *J. Am. Chem. Soc.* **1989**, *111*, 4324.
(4) Haga, M.; Dodsworth, E. S.; Lever, A. B. P. *Inorg. Chem.* **1986**, *25*, 447.
(5) Haga, M.; Isobe, K.; Boone, S. R.; Pierpont, C. G. *Inorg. Chem.* **1990**, *29*, 3795.
(6) Bhattacharya, S.; Boone, S. R.; Fox, G. A.; Pierpont, C. G. *J. Am. Chem. Soc.* **1990**, *112*, 1088.
(7) Boone, S. R.; Pierpont, C. G. *Polyhedron* **1990**, *9*, 2267.
(8) Bhattacharya, S.; Pierpont, C. G. *Inorg. Chem.* **1991**, *30*, 1511.
(9) Bhattacharya, S.; Pierpont, C. G. *Inorg. Chem.* **1991**, *30*, 2906.
(10) Bradbury, J. R.; Schultz, F. A. *Inorg. Chem.* **1986**, *25*, 4416.
(11) Abbreviations: BQ, SQ, and Cat have been used to refer to benzoquinone, semiquinone, and catecholate forms of the quinone ligands, Q has been used to refer to quinone ligands of unspecified charge, and DB- and Cl_4- have been used as prefixes for the 3,5-di-*tert*-butyl- and tetrachloro-substituted quinone ligands.
(12) Lever, A. B. P.; Auburn, P. R.; Dodsworth, E. S.; Haga, M.; Liu, W.; Melnik, M.; Nevin, W. A. *J. Am. Chem. Soc.* **1988**, *110*, 8076.
(13) Jackson, L. C.; MacLaurin, R. D. *J. Am. Chem. Soc.* **1907**, *37*, 11.

0020-1669/92/1331-0035$03.00/0